ADMET & DMPK 6(2) (2018) 85-104; doi: ***http://dx.doi.org/10.5599/admet.529***

ADMET

Open Access : ISSN : 1848-7718

http://www.pub.iapchem.org/ojs/index.php/admet/index

Review

Leveraging chromatography based physicochemical properties for efficient drug design

Gilles H. Goetz*, Marina Shalaeva

Molecular Properties Group, Worldwide Medicinal Chemistry, Pfizer Worldwide Research & Development, Pfizer, Inc., Groton, Connecticut 06340, United States

*Corresponding Author E-mail: gilles.h.goetz@pfizer.com; Tel.: +1-860-715-6311

Received: March 28, 2018; Revised: May 26, 2018; Available online: June 04, 2018

Abstract

Applications of chromatography derived lipophilicity, polarity, and 3D concepts such as conformational states, exposed polarity and intramolecular hydrogen bonds (IMHB), are discussed along with recently developed methods for incorporating these concepts into drug design strategies. In addition, the drug design process is described with examples and practices used at Pfizer, as well as experimental and computed parameters used for parallel optimization of properties leading to drug candidate nominations.

Keywords

ElogD, EPSA; lipophilicity, exposed polarity

Introduction

An active molecule with favorable pharmacokinetic/pharmacodynamic (PK/PD) properties is the goal of drug design. This means a biologically active molecule can be developed into a drug only if it fits strict pharmacological profile requirements. Tablets are the preferred form of administration due to convenience, patient compliance and ease of manufacturing. Therefore most drug design projects are focused on creating drugs suitable for oral dosage.

In order to be absorbed in the gastrointestinal (GI) tract, a solid formulation must be ingested, solubilized. Only then can the solvated drug be absorbed into the blood stream. Here drug distribution, metabolism and excretion affect its clearance, defining the pharmacokinetic parameters, half-life and Therapeutic Index (TI). Balancing Absorption, Distribution, Metabolism, Excretion and Toxicity (ADMET) properties is a major challenge in drug discovery and development. Failure to achieve the right ADMET balance was cited in 1997 as the reason for the attrition of 40% of drug candidates during development [1]. Here we present and discuss recent advances and approaches, mostly developed at Pfizer, using chromatographically determined physicochemical properties for the optimization of ADMET properties.

Lipophilicity

Lipophilicity (as defined by IUPAC) represents the affinity of a molecule or a moiety for a lipophilic environment. It is commonly measured by its distribution behavior in a biphasic system, either liquid-liquid

(partition coefficient between 1-octanol and water) or solid-liquid (retention on reversed phase high performance liquid chromatography (RP HPLC)) [2]:

Lipophilicity may be expressed as log *P* for neutral molecules and log *D* for ionized molecules at a particular pH (log D_{pH}), where permeation *P* and distribution *D* are defined by the neutral and ionized species concentration ratios:

$$P = \frac{[\text{neutral}]_{\text{octanol}}}{[\text{neutral}]_{\text{water}}} \qquad D = \frac{[\text{ionized + neutral}]_{\text{octanol}}}{[\text{ionized + neutral}]_{\text{water}}} \ .$$

Successful drug designs require careful balancing of *in vivo* and *in vitro* properties. Lipophilicity is a descriptor intrinsic to many of these properties. Computational models of ADMET properties generally include log *P* as a significant descriptor of the modelled parameter.

An extensive analysis of the literature linking ADMET and lipophilicity in drug discovery was published by Waring [3]. It details important, but obscure aspects of the log *D* parameter. For example, many studies rely on compilations of log *P*/log *D* values from a variety of sources with poorly described experimental details. These non-homogeneous datasets lead to discrepancies in analyses. There is also confusion between log *P* and log *D*; terms often used interchangeably.

For drug compounds ionized at physiological pH, log D_{pH} is more relevant than log *P*, however, it deviates because of its dependence on p*K*a. This is especially flagrant, in case of predicted log D_{pH} , due to unreliable p*K*a predictions. The widely cited publication by Mannhold *et al*. [4] compares several computed log *P* models to over 96,000 measured values. Unfortunately, actual experimental details were not provided.

Many research organizations have developed their own methods for lipophilicity measurements. They use their particular values for drug design and optimization, i.e. chromatographic hydrophobicity index (CHI) at GlaxoSmithKline [5], and Elog *D* at Pfizer [6].

Early stage drug design strives to create the most active molecule for a particular therapeutic target. The ultimate goal is the discovery of a molecule possessing “drug-like” properties. The reliance on lipophilicity to understand molecules' drug-like properties was defined in 1997 Lipinski's “rule of five” (Ro5) [7]. Now it is ingrained into drug design that oral drugs require a cLogP < 5. Rules, depending mostly on log *D*, help guide designs towards optimal drug-like chemistry space. Log *D* is used to calculate ligand efficiency (LE) [8,9], metabolic efficiency (MetE) [3,10,11], central nervous system multiparameter optimization (CNS MPO) [12,13], and toxicity scores [14-16].

Recent developments are reviewed in the application of log *D* for balancing potency and ADME properties.

Lipophilicity and ligand efficiency

The review by Hopkins *et al*. [17] concluded that recently marketed oral drugs “frequently have highly optimized ligand efficiency values for their targets”. Early stage design efforts often lead to series of hundreds of newly synthesized compounds. These structures need to be rapidly evaluated for projects to proceed. Promising leads may be prioritized using lipophilic ligand efficiency (LLE) [9] or LipE [10]:

LLE (or LipE) = pIC_{50} – cLogP .

The LLE/LipE concept has been developed following the introduction of ligand efficiency (LE) [8]. The LE parameter allows direct comparison of molecules through their target binding energy. LE can be expressed

by the following simplified equation in which N is the number of non-hydrogen atoms:

$LE = 1.37(-\log IC_{50})/N$.

Project progress may be tracked using both LE and LipE; LipE is expected to reach values of 6 or 7 for a potential drug candidate to be chosen for further development [18-20].

Target binding increases with the addition of a lipophilic fragment, at the expense of potential for off-target binding and decreased solubility. An efficient drug design requires potency to be achieved with a minimal increase in MW or lipophilicity [21-24].

Lipophilicity and oral absorption

Oral administration, the most desirable route of medicine delivery, requires a drug to be absorbed while in the GI tract, with cell membrane permeation being the major determinant of absorption.

There are several processes involved in crossing the intestinal mucosa, including active transport [15], paracellular transport, and drug efflux. Passive membrane diffusion is considered to be the major contributing process [25]. Recent analyses continue to demonstrate the significance of the non-specific permeation mechanisms governed by molecular properties (namely molecular size and polarity) [16].

The favorable property space for an orally administered drugs is defined by the afore mentioned Ro5 [26,27]. In order to achieve absorption, an oral drug needs to have a cLogP < 5; MW < 500; hydrogen bond donor (HBD) count (NH+OH) < 5; and a hydrogen bond acceptor (HBA) count (N+O) < 10.

More specific rules were developed for central nervous system (CNS) projects, where crossing the blood-brain barrier is challenging due to tighter junctions and higher efflux. The CNS MPO score introduced by Wager *et al*. [12] was derived by analysis of drugs and candidates with regard to their ability to cross the blood-brain barrier. The CNS MPO includes ionization constant (p*K*a), log *P*, and log $D_{7.4}$. This emphasizes the importance of ionization and lipophilicity adjusted for ionization [13,23,28,29]. Recently Z. Ranković further refined the CNS desirability criteria in CNS MPOv.2 [30].

Lipophilicity measurements also help to estimate solubility in discovery settings [31]; solubility decreases with log *P* > 3.

Current trend towards and beyond Ro5 compounds

Recently, the introduction of innovative “flat” targets and the potential for higher potency and selectivity provided by larger molecules, has led to a renewed interest in peptide-based drugs. These fill the gap between small molecules and biotherapeutics, as illustrated in Figure 1 [32,33].

The exploration of new targets required new design concepts including “an update” to Ro5. Bunnage *et al.* defined "four pillars of target validation”, the first pillar being “exposure at the site of action”, defined largely by permeability, where tactics such as increasing lipophilicity could help improve both potency and permeability [34].

Failing one or more of the Ro5 may decrease oral bioavailability, due to low solubility, and or poor membrane permeability, in addition to metabolic instability, synthetic complexity and other disadvantages of large drug molecules.

The study by Guimarães *et al.* [35] highlighted the importance of 3-D properties for passive permeation of beyond Ro5 (bRo5) molecules, where taking molecular conformation into account, as well as size and polarity assessments, are needed to aid design in bRo5 space.

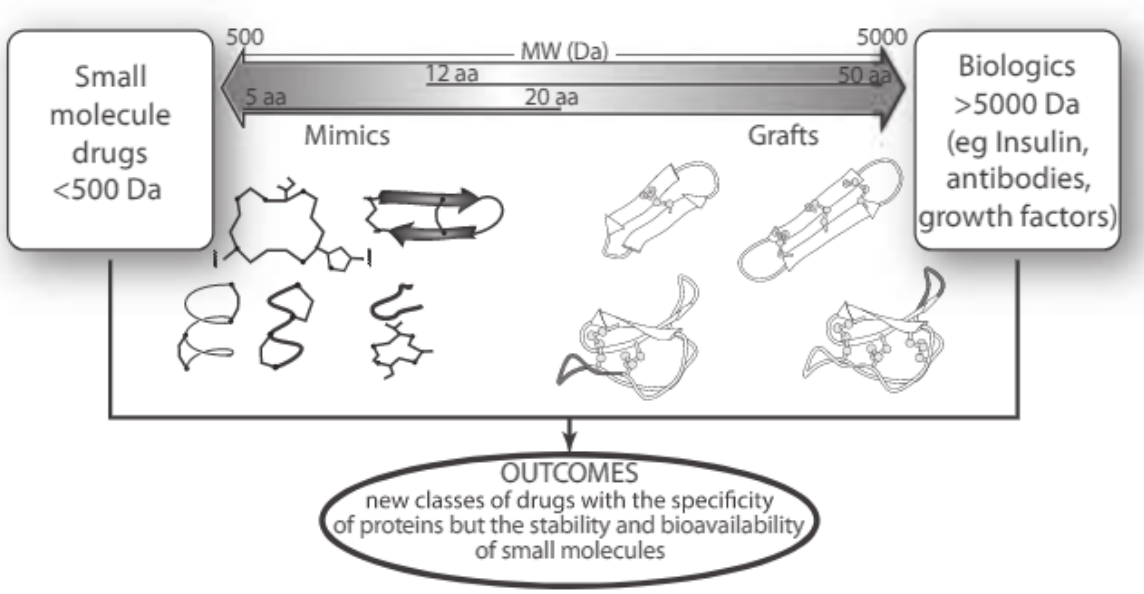

Figure 1. Schematic illustration of the molecular weight (MW) gap between conventional small molecule drugs (< 500) and biologics (> 5000). Reprinted from [32] Copyright (2013), with permission from Wiley.

The Ro5 defines properties of drug-like molecules, essentially, via molecular size and polarity, where MW describes the size, HBD and HBA counts describe polarity and log *D* describes both. Notably, MW and NH, OH, O and N are just simple counts and only roughly describe interactions with the environment, especially for molecules of any complexity. For example, intramolecular hydrogen bonding (IMHB) in large, flexible molecules could lead to shielding of HBD and HBA and, consequently, to changes in molecular shape and size, which are not accounted for by MW or HBD and HBA counts. These simple counts, including polar surface area (PSA), are indifferent to changes in molecular shape and size, the major determinants of passive diffusion [35].

Experimental log *D*, on the other hand, accounts for molecular size and polarity in solution and for 3D conformational changes adopted by the molecule. Therefore, the "extension" of the Ro5 to large molecules depends even more on the "effectiveness" of the log *D* parameter. While the accuracy of log *D* prediction is important for large, flexible molecules, it is also much more difficult to predict, as it deals with the assessment of multiple conformations and their populations. Measured log *D* values are necessary to build and test such computational models for bRo5 compounds. However, log *D* values > 3 are challenging to obtain via conventional shake-flask log *D* (SFlog *D*), due to limits in quantitation for the concentration of above 1000 between phases.

Kihlberg *et al*. analyzed orally available drugs in bRo5 space [36] and observed significant extension, almost doubling in values of Ro5 parameters (Figure 2). They proposed an "extended Ro5 space" (MW < 700, 0 < cLogP < 7.5, HBD < 5, PSA < 200 Å^2, and the number of rotatable bonds (NRotB) < 20. They also proposed a substantially larger ''possible to be oral" bRo5 space with the limits for oral bioavailability extended to approximately MW < 1000, -2 < cLogP < 10, HBD < 6, HBA < 15, PSA < 250 Å^2, NRotB < 20 (dashed box). Notably, HBD has hardly changed (increased by only 1 count) highlighting the significance of limiting HBD exposure for oral absorption of large molecules.

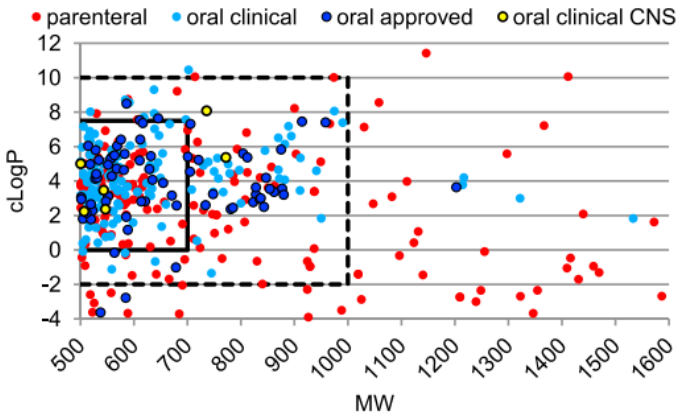

Figure 2. Physicochemical property space of drugs and clinical candidates with MW > 500. Solid box marks "extended Ro5" space. Dashed box marks "bRo5" space. Reprinted from [36] Copyright (2014), with permission from Elsevier.

Wang *et al*. [37] observed a correlation of RP HPLC log *k*' with passive permeability determined by human colorectal adenocarcinoma cells (Caco-2) and the parallel artificial membrane permeability assay (PAMPA) for a set of macrocyclic peptides. Bockus *et al*. used Elog *D* (5.5 to 7.5) to study macrocycles. The lipophilicity values correlated with cell-based permeability values by Madin-Darby canine kidney (MDCK)-low efflux cells (MDCK-LE) [38].

Lokey *et al*. investigated Ro5 and bRo5 compounds with MW > 1000 and demonstrated a sharp decline in apparent passive permeability for compounds with molecular size above 750 Å [39]. They also concluded that bulk physical properties contributing to passive permeability could be approximated by lipophilicity and molecular size (log $K_{hydrocarbon/water}$ and MW respectively). Molecular size relates to passive permeability with p*K*a and aqueous solubility also very important properties to consider. The lipophilicity parameter used by Lokey *et al*. (log $K_{hydrocarbon/water}$) is lipophilicity measured in a non-polar environment and is different from log $D_{octanol/water.}$ It has been shown to correlate well with passive permeability measured by PAMPA and MDCK-LE.

The use of Δlog *P* = log $P_{alkane/water}$ – log $P_{octanol/water}$ was first introduced by Seiler [40] and applied to improve absorption [41], as a guide in the design of novel brain-penetrating H2 antagonists [42], or as a measure of HBD acidity [43,44]. Hydrogen bonds characteristically feature binding energies and contact distances that can lead to large variations even for a single donor-acceptor pair [45].

The 96-well plate-based shake-flask log $P_{toluene/water}$ method (pH 1 to 11) was developed along with the IMHB interpretation scheme based on Δlog *P* [46]. This method allows verification of molecular conformations predicted by COSMO-RS software [47] which describes the geometry of virtual molecules' interactions in both polar and non-polar environments.

Furthermore, an RP HPLC method using a polystyrene-divinylbenzene stationary phase (PLRP-S) was developed to simulate a non-polar lipidic membrane environment [48], and to obtain experimental lipophilicity values.

Kihlberg et al described errors in cLogP; log P_{oct} predictions that were far from the experimentally determined values [36]. Posaconazole has a cLogP of 5.4, while the experimentally determined log *P* is 2.4 [49]. However, in this particular case, the measured value may be incorrect.

These studies reiterate the need for an extended range of lipophilicity measurements for bRo5 compounds that would accommodate the large lipophilic molecules designed for current targets. They highlight the importance of lipophilicity as an approximation of molecular size and conformations in specific environments.

Lipophilicity and Clearance

Avoiding highly lipophilic compounds is a design principle used to improve clearance [50]. The analysis of matching pairs conducted by Stepan *et al*. [11] confirmed that changes in metabolic stability largely come from changes in lipophilicity (Figure 3). To determine how structural changes affect the relative clearance between analogues, the lipophilic metabolism efficiency parameter (LipMetE) was introduced. LipMetE relates lipophilicity to the *in vitro* metabolic clearance measured by the human liver microsomes (HLM) assay. LipMetE and unbound clearance ($CL_{int,u}$) are defined as follows:

$$\text{LipMetE} = \log D_{7.4} - \log (CL_{int,u}) \ ,$$

$$CL_{int,u} = CL_{int,app}/f_{u,mic} \ .$$

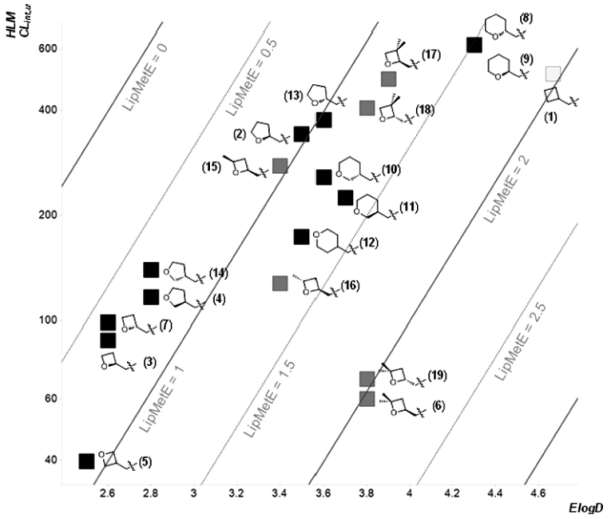

Figure 3. The plot of unbound clearance, $CL_{int,u}$, versus experimental log *D*, Elog *D*. The 45° lines represent different values of LipMetE. Compounds that parallel the same 45° line offer the same ratio of metabolic clearance to lipophilicity. Reprinted with permission from [11]. Copyright (2013) American Chemical Society.

Stepan *et al.* [11] suggested choosing high LipMetE compounds as a starting point for optimization due to their wider LogD range. Thus, potency and permeability could be improved while maintaining low clearance. LipE and LipMetE have become complementary opposites ("yin and yang") in medicinal chemistry decision making at Pfizer and the authors provide specific guidance on simultaneously optimizing these lipophilicity driven parameters.

Optimization of ADME properties, such as cell membrane permeability and metabolic stability, often comes to an act of balancing these orthogonal parameters. Gleeson [14] describes the contribution of MW, ionization state, and cLogP to *in vivo* clearance. Log clearance (log Cl) was largest for a cLogP > 5, less pronounced for cLogP 3–5, and most favorable for a cLogP < 3. Johnson *et al.* [16] analyzed permeability and clearance data for 47,018 Pfizer compounds and observed broad trends for favorable clearance and permeability compared to MW and log *D*. Using lipophilicity determination, they identified a "golden triangle" of MW and log *D* values for optimal permeability and metabolic stability. Figure 4 shows permeable and stable compounds in blue and compounds failing permeability or metabolic stability in grey against MW and log *D*. Compounds with favorable clearance and permeability properties are clustered within this "golden triangle" of MW and log *D*.

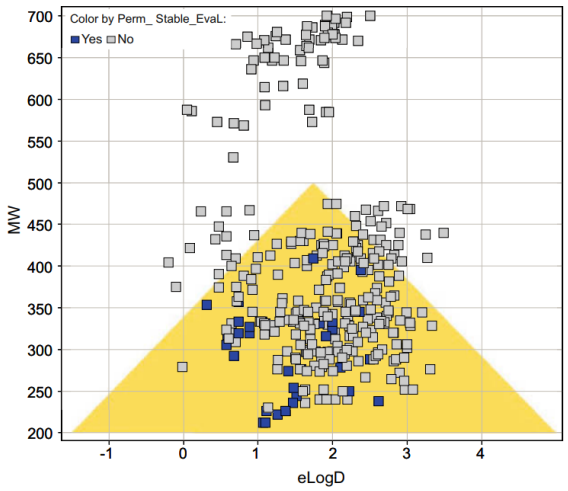

Figure 4. Combined *in vitro* permeability and clearance trends across MW and log *D*. Reprinted from [16] Copyright (2009), with permission from Elsevier.

Lipophilicity and Toxicity

Avoiding high lipophilicity is also critical for reducing the probability of adverse safety findings [3, 51]. Hughes *et al.* [52] demonstrated that lipophilic compounds (cLogP > 3) with a low polar surface area (PSA < 75 Å^2) have a 6-fold greater risk of toxicity findings in preclinical toxicology studies [53].

An alternative to using log *P*, which could oversimplify *in vivo* behavior of compounds, was proposed by Wenlock [54]. This criterion is based on the amount of compound in the body at a steady state. The relationship of this criterion at an acceptable human dose of 0.5 mg/ kg for 242 oral drugs with different *in vivo* plasma clearances was established with regard to their safety profiles.

Experimental log D determinations

The optimal range of log *D* to satisfy ADMET properties centers on 2 (+/-1) [3], but expands far beyond that range for some marketed drugs [36]. The wide range of lipophilicity employed in modern drug design requires experimental methods and computational models to support exploitation of these chemical spaces.

The chromatography based Elog *D* method [6, 55] has been developed at Pfizer to alleviate limitations the of the classical shake-flask technique and to extend to compounds bRo5. Since its introduction, it has been used successfully in a traditional chemistry space [22, 56-60] as well as in the bRo5 programs [38].

The simultaneous optimization of potency and clearance using both measured and calculated Elog *D* has been described for the Takeda-G-protein-receptor-5 (TGR5) program seeking an orally available compound for improved glycemic control via glucose-dependent insulin secretion. This has led to significantly improved clearance (HLM < 100), log *D* = 2, and equivalent potency compared to competitor compounds with high clearance HLM > 200 and log *D* > 2 [50].

Lipophilicity (Elog *D*) has also been utilized in clinical studies to understand the specific and non-specific binding of an active ingredient to the beta-amyloid plaques in Alzheimer's disease patients which has been observed with high contrast positron emission tomography (PET) imaging [61].

At Pfizer, log *D* at pH 7.4 is routinely measured for most compounds using either SFlog *D* or Elog *D* or both methods; each method has limitations. While Elog *D* cannot be applied to acids, SFlog *D* has a limitation in measuring values above 3.5 due to the increasing errors in quantification of concentration

extremes (indeed, log *D* = 4 implies that the concentration in 1-octanol is 10,000 times higher than in the aqueous phase). Additionally, an accurate prediction of log *D* at pH = 7.4 is still an issue for novel structures and therefore comparisons of SFlog *D* and Elog *D* values are often useful.

With project X, compounds were evaluated using SFlog *D* (and occasionally Elog *D*), but significant discrepancies were observed for "low" SFlog *D* samples (Figure 5. (a)). However, if Elog *D* – SFlog *D* differences (residuals) were plotted against Elog *D* it became apparent that the largest discrepancies were in the range above 3.0. (Figure 5(b)). This illustrates how the SFlog *D* procedure may underestimate lipophilicity values above 3.

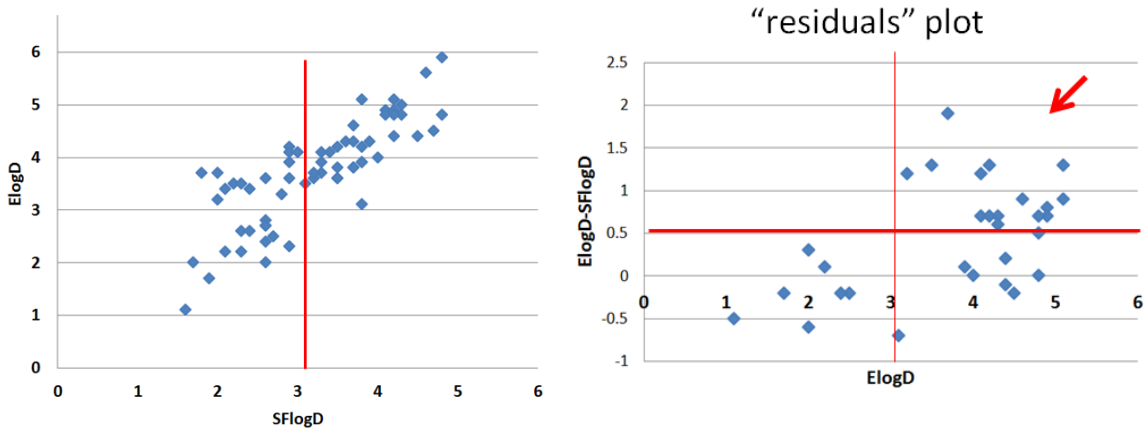

Figure 5. (a) Comparison of SFlog *D* and Elog *D* values for project X; **(b)** SFlog *D* - Elog *D* residuals vs. Elog *D*

In summary, if analyzed by Elog *D*, both SFlog *D* and Elog *D* give, as expected, very similar values (within +0.5) in the Elog *D* < 3 range. However, in the Elog *D* > 3 range, many SFlog *D* values are under-evaluated (by up to 2 log units). Therefore, it is important to recognize and respect the experimental methods applicability domain when using log *D* for SAR or building computational models based on such data.

Computed log D

Day-to-day experience in measuring log *D* demonstrated that despite great efforts to improve log *D* calculations, there were still instances where log *D* predictions are inaccurate; especially if ionization is involved and an accurate p*K*a is needed to adjust the calculated log *P* of a neutral form to a log *D* at a particular pH, usually 7.4.

The cPFLogD model built at Pfizer takes into account both SFlog *D* and Elog *D* experimental values while respecting the limits of each method, i.e. SFlog *D* < 3 and Elog *D* for bases and neutrals only. Consequently, the model gives preference to SFlog *D* values in the log *D* range below 3 and to Elog *D* values in the log *D* range above 3. The cPFLogD model is built using the Cubist non-linear in-silico regression methodology and it is regularly updated with the latest experimental data, thus providing improved cPFLogD predictions for the next design cycle.

Performance of the cPFLogD model is demonstrated in Figure 6 on a rather challenging subset of diverse "natural-product" like compounds. This subset of about 300 molecules is more complicated than encountered in most small molecule projects. It encompasses MW from 200 to 2000, has compounds violating up to four Ro5, with high NRotB, HBD and HBA.

For many compounds in the log *D* > 4 range a SFlog *D* value could not be acquired due to extremely low concentration in the aqueous phase and therefore Elog *D* values were measured on all compounds, excluding acids.

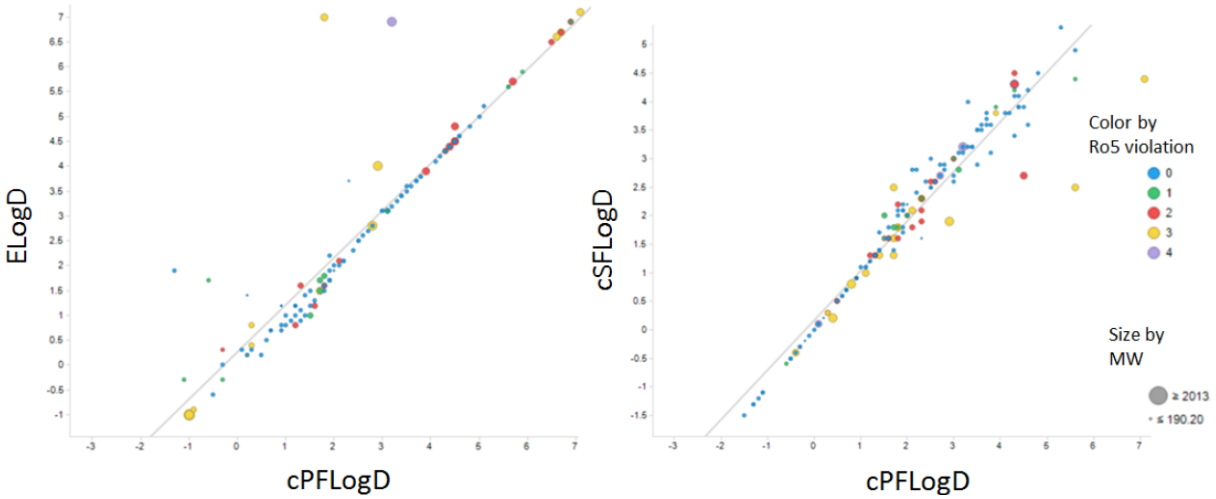

Figure 6. (a) Measured Elog *D* vs. cPFLogD; **(b)** Measured SFlog *D* values vs. cPFLogD. A diverse subset of "natural product"-like library, about 300 compounds. The size of the markers represents Molecular Weight (193 to 2013 Da). The colours represent violations of the Ro5.

As expected, cPFLogD predicted SFlog *D* more accurately in the < 2 range and, Elog *D* more accurately in the > 2 range. Several outliers in the upper left corner of the Elog *D* vs. cPFLogD Figure 6(a) represent the underestimated SFlogD results used by the cPFLogD model leading to underestimated prediction values.

Comparison of cPFLogD to commercially available ACDlabs log $D_{7.4}$ predictions for the same subset are shown in Figure 7, where many compounds violating three Ro5 criteria (yellow markers) fell far outside cPFLogD, especially in the low lipophilicity range.

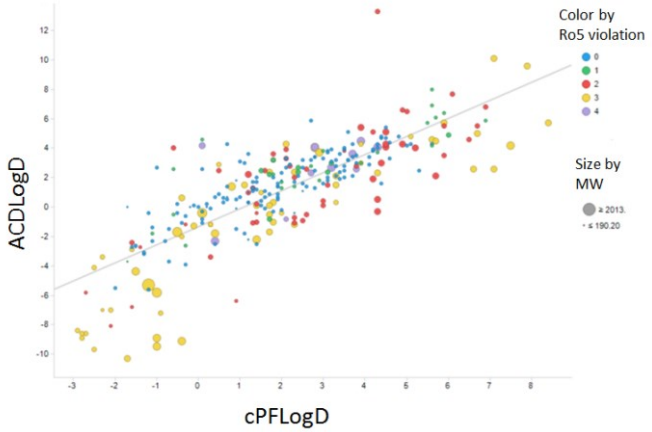

Figure 7. Lipophilicity calculations using log $D_{7.4}$ by ACD labs vs. cPFLogD for a subset of a "natural product"-like library.

It should be emphasized that project teams usually design around an active lead molecule and work on a few series, where "diversity" in a general chemistry sense is rather limited. Therefore, measured log *D* values determined on a few compounds in a series introduced into the model often allow significant improvement in accuracy of cPFLogD predictions in that chemical space.

Polarity

In the otherwise comprehensive IUPAC Compendium of Chemical Terminology, also known as the Gold Book, (unlike lipophilicity, hydrophobicity and hydrophilicity), the compound polarity is not defined [2]. The only reference to polarity in the Gold Book is coupled with the concept of solvent rather than solute (see below).

When applied to solvents, the term polarity covers their overall solvation capability (solvation power) for solutes (i.e. in chemical equilibria: reactants and products, in reaction rates: reactants and activated complex, in light absorptions: ions or molecules in the ground and excited state). A solvent's solvation power depends on the action of all possible intermolecular interactions between solute ions or molecules and solvent molecules. Those interactions can be both nonspecific and specific but exclude the interactions leading to definite chemical alterations of the ions or molecules of the solute.

TPSA

In the context of drug design, the polarity of a molecule has been redefined as its polar surface area (PSA). Originally computed using molecular mechanics calculations, the fragments of the dynamic van der Waals' surface area associated with oxygen, nitrogen and their attached hydrogen atoms were considered as the polar portions of the molecular surface area. This showed correlation to cell permeability in Caco-2 cells for a homologous series of beta-adrenoreceptor antagonists [62].

The popularity of PSA has recently increased significantly, due to its performance in predicting intestinal adsorption as well as blood-brain barrier penetration [63-70].

In 2000 Ertl *et al*. introduced the topological polar surface area (TPSA)[71], an index based on the addition of tabulated surface contributions of polar fragments. Based on ~35.000 drug-like molecules, the surface contributions of 43 fragments centered on polar oxygen, nitrogen, phosphorus and sulfur were determined by the least square fit and tabulated. This methodology proved 2-3 orders of magnitude less computationally intensive than the previous PSA calculations and gave similar results [71]. The use of PSA in medicinal research has since been reviewed by Ertl [72].

In addition to dynamic, molecular and topological polar surface areas, quantum mechanical polar surface area (QMPSA) was recently introduced and showed a good correlation with the fraction absorbed (FA) after oral administration for a set of 18 drugs when carboxyl groups were deprotonated, suggesting adsorption to be strongly related to polar interactions of molecules in water solution [73]. It should be noted that significant increases in computing resources are needed to generate QMPSA, compared to the table-entry recalling TPSA.

While mostly used for barrier crossing prediction in an ADME context, TPSA has also been recently investigated as a descriptor for 2D-QSAR for diverse pharmacological activity data [74], as well as for active drug transport by multidrug resistance associated protein 1 (MRP1) [75].

The first study pointing to a hard PSA limit dates back to 1997, in which Palm *et al*. [65] showed on a diverse set of 20 model drugs, that fully absorbed drugs (FA > 90 %) had a PSA ≤ 60 $Å^2$ while drugs that are less than 10 % absorbed had a PSA > 140 $Å^2$. Later, Veber at all [76] showed that a PSA ≤ 140 $Å^2$ and the number of rotatable bonds ≤ 10 is as efficient and selective a criterion as the Lipinski's Ro5 for selecting oral bioavailability of > 20-40 %. As far as the blood-brain barrier was concerned, it was found that the upper limit for PSA for a molecule to penetrate the brain was around 90 $Å^2$ [69,77].

TPSA in MPO

In 2010 Wager at al introduced the CNS MPO (multiparameter optimization) desirability tool, which incorporated TPSA along with 5 other fundamental physicochemical properties: cLogP, cLogD, MW, p*K*a, and HBD. A monotonic decreasing function was used for cLogP, cLogD, MW, p*K*a, and HBD, and a hump function was used to define TPSA (Figure 8). The CNS MPO desirability method is quite simple, with parameters derived from medicinal chemistry best practices, and it is able to balance multiple variables

while avoiding hard cut-offs. It demonstrated a good correlation between a high score (> 4 out of a possible max of 6) and good *in vitro* ADME properties [12,78].

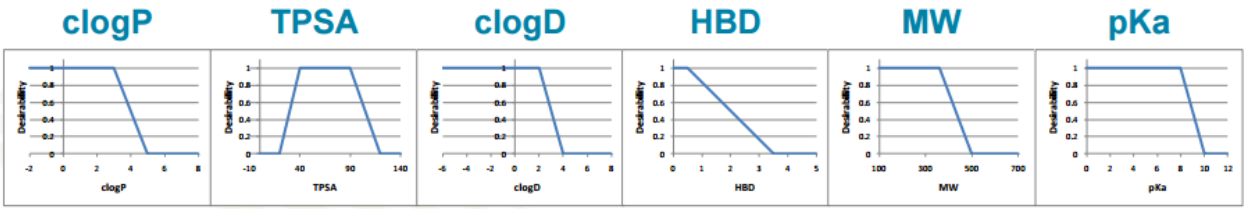

Figure 8. Components of CNS multiparameter optimization desirability tool (MPO)

EPSA

Having access to TPSA, a simple, inexpensive and efficient way to assess polarity from a 2D structure, which correlates reasonably well with cell permeability, the need for a polarity measurement was never really felt by drug design professionals.

While historically relevant for the targets pursued in the late 1990s, criteria such as the Ro5 or the Veber PSA-Rotatable bonds rule [76], tend to lose traction due to the rarity of easy targets, resulting in drug discovery programs having to foray into more challenging chemical spaces. In Jürgen Drews' words "one truth is there for all to see: many 'easy' targets or molecules have been found and developed" [79].

Over the time, simplification of the polar surface area calculations down to TPSA may have led to the false equivalency of certain considerations such as the actual position of a polar group in a molecule with regard to its immediate and adjacent environment. For example, the TPSA values for ortho-, meta- and para- analogues of any aromatic polar compound are identical, and similarly, the TPSA values of any regioisomers are also identical, due to the nature of the TPSA calculation, solely based on adding fragment contributions to overall polarity. We contend here that each polar fragment does not contribute equally to the polar surface area of a molecule; in essence advocating a return to a more "3D-PSA"-like descriptor [35,62].

Utilizing separation sciences expertise, a team of Pfizer scientists developed an assay which outputs a polarity readout termed EPSA (not an acronym) [80]. The main driver behind EPSA was to have access to a fast, robust method capable of identifying the potential for a compound to form intramolecular hydrogen bonds (IMHB) enabling it to hide polarity that might otherwise reduce its passive permeability. Indeed, the identification of compounds likely to form IMHBs is an important drug design consideration given the correlation of intramolecular hydrogen bonding with increased membrane permeability [81-85].

The EPSA method provides, under controlled supercritical fluid chromatography (SFC) conditions, an exposed/hidden polarity readout that is derived from the retention time of a compound on a specific column. The stationary phase, (Phenomenex Chirex 3014) was selected for its balance of lipophilic and polar attributes and its capacity to separate compounds with wide polarity differences. SFC, which essentially uses normal phase-like conditions, provides an environment with a low dielectric constant conducive to IMHB formation. Polar compounds are retained more under these conditions, and a low-slope gradient of methanol achieves elution based on the increasing polarity of the mobile phase. In the cases that have been studied, using matched molecular pairs with or without IMHBs, compounds with IMHB resulted in a significant reduction in polarity and eluted earlier in the chromatogram. Results are normalized through the use of calibration standards generating a linear relationship between retention times and EPSA values [80].

This is possible to confirm or disprove the presence of an intramolecular hydrogen bond (IMHB) in small

molecules or peptides using EPSA and pairwise analysis. Such IMHBs are a critical factor affecting the conformation of molecules and can have a direct impact on their absorption into the human body, their permeability into target cells, and even their potency against therapeutic targets.

This method has been successfully used in a small molecule medicinal chemistry project to assess exposed polarities of their lead compounds. Cheng *et al*. [86] determined EPSA for their mechanistic target of rapamycin (mTOR), phosphatidylinositol-3 kinase (PI3K) dual inhibitors series and found no direct correlation between EPSA and TPSA. However, they showed that the formation of IMHB can significantly reduce the effective polar surface area. Suggesting that for designs with high TPSA, the introduction of an IMHB can help achieve good permeability and cellular potency by modulating the EPSA to a desirable range. Indeed, several compounds, with TPSA greater than 135 Å^2, exhibit EPSA values between 82 and 101, which is a range capable for this series of yielding permeability and cellular potency.

Wakenhut *et al*. [87] determined EPSA for non-structural protein 5A (NS5A) inhibitors and notably compared two analogues: **12** and **13**. Compound **12** has less HBD and HBA, less rotatable bonds, lower TPSA (105 Å^2) and, by all standard medicinal chemistry principles, **12** was expected to be more permeable than **13** (TPSA 175 Å^2). It turned out that the opposite was true; compound **12** was not permeable while **13** was permeable. Compound **12** had an exposed polarity value (EPSA) of 128, while the EPSA value of **13** was 103, significantly lower than for **12**.

These facts can be explained by the peripheral functionality capable of forming IMHBs in **13** within a membrane environment, thereby masking H-bonding (HBD and HBA) character and contributing to passive permeability, as compared with the more extended conformations available to compounds such as **12** incapables of forming IMHBs (Figure 9). The team based its subsequent designs on enabling IMHB formation within the analogues being developed.

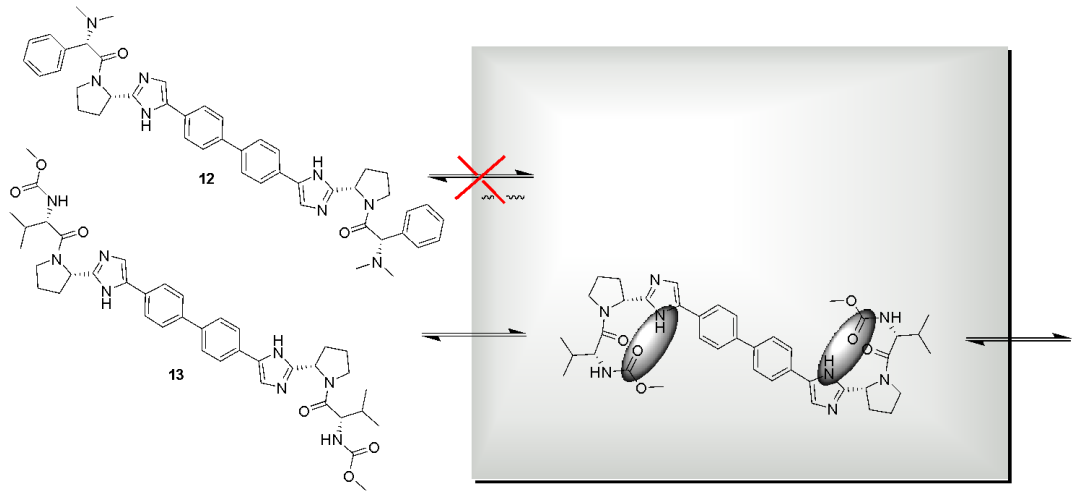

Figure 9. Representation of compound **12** and **13**. Compound **13** initially in solution phase (6 HBA, 4 HBD, PSA = 175 Å^2) and as it traverses a hydrophobic membrane (4 HBA, 2 HBD, 3D-PSA~120 Å^2) as a possible explanation of the good membrane permeability of **13**. Adapted from [87] Copyright (2014), with permission from Wiley.

EPSA and Peptides

Once EPSA was established as a viable polarity monitoring tool for small molecules, its remit was expanded to peptides, notably cyclic peptides, which have generally demonstrated insufficient permeability to be used as oral drugs. Guiding the design of such peptides without a reliable permeability monitoring method is a challenge. Since for peptides, the main obstacle to permeability is polarity, the EPSA experiment was a perfect fit.

Goetz *at al*. [88] have reported a project team design strategy illustrating the suitability of EPSA as a surrogate for cyclic peptide permeability. While working towards improving permeability of their lead compounds, the team was faced with a flat structure-permeability relationship (no significant improvement in permeability as measured by RRCK cells was detected with any modification). Since the lead compound had an EPSA value in the high 160s, reducing measured polarity became the surrogate objective. EPSA measurements drove each new design. Plans that increased EPSA were abandoned in favor of those decreasing EPSA. With each design cycle it was observed that a gradual decrease in polarity was obtained but without any significant improvement in permeability as measured by RRCK, until a threshold in EPSA was reached (EPSA < 100) upon which permeability became measurable and increased to reach acceptable levels (EPSA < 80).

At Pfizer, and across multiple academic collaborations [38,89-91], project teams routinely use EPSA data to inform peptide design as a predictor of permeability and as an indicator of IMHB patterns in cyclic peptides. Furthermore, EPSA is now used in a prospective way after the development of an in-house computational model [92]. It was built using the following procedure. Compounds undergo a thorough conformational analysis (Macro model) followed by 3D descriptors calculation (VolSurf+) based on molecular interaction fields (MIFs). A partial least squares (PLS) regression algorithm is then used to establish a quantitative relationship between the matrix of descriptors and the EPSA endpoint. Implementation of the computational EPSA prediction model, combined with other physicochemical properties, has enabled virtual compound design, selection of better candidates for synthesis and has accelerated efficiency of design cycles.

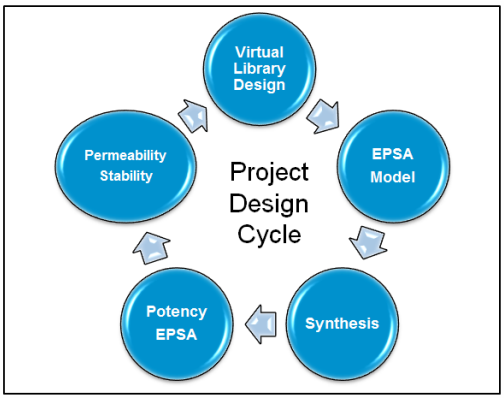

Figure 10. Illustration of polarity based design cycle enabled by the Pfizer computational EPSA prediction model

In the particular example depicted in Figure 10, the computational EPSA prediction model was successfully implemented by the project team, first designing virtual compound libraries, and then testing their EPSA predictions, as a permeability surrogate. Only compounds with predicted EPSA values < 95 were prioritized for synthesis. Compounds with reasonable potency and measured EPSA < 100 were prioritized for cell-based passive permeability evaluation and HLM stability assessment. Learnings from this data the next design cycle was refined [93].

The EPSA technique and its application are not reserved or limited to Pfizer and its collaborators, indeed, EPSA has been implemented across the pharmaceutical industry, i.e. at AbbVie [94], Novartis [95], and Merck [96], EPSA services are available through an established analytical CRO [97]. Additionally, Peter Wipf in his January 2017 editorial [98] selected EPSA as one of the 6 technical innovations published in ACS Medicinal Chemistry Letters over the past 3 years that facilitate the practice of medicinal chemistry and are likely to become essential items in the medicinal chemist's toolbox.

Conclusions

Across the pharmaceutical industry, each R&D department has its own philosophy. Based on historical approaches, resource allocations and leadership advocacy, drug design strategies essentially follow the same guidelines with regards to lead optimization: exquisite potency along with favorable ADMET profiles in the least amount of time and at the lowest possible cost. Guiding those design strategies through chromatography based physicochemical properties (i.e. Elog *D* and EPSA) is one of the more successful approaches developed in order to accelerate the process.

***Acknowledgements**: Laurence Philippe for her continuous support and mentorship, Patrick Mullins and Jason Ramsay for critical editing and Justin Montgommery for Figures 6 and 7.*

References

[1] T. Kennedy. Managing the drug discovery/development interface. *Drug Discov Today* **2** (1997) 436-444.

[2] A.D.W. McNaught, M. Nic, J. Jirat, B. Kosata, A. Jenkins. IUPAC. Compendium of Chemical Terminology, 2nd ed. IUPAC the "Gold Book", Blackwell Scientific Publications, Oxford 2006.

[3] M.J. Waring. Lipophilicity in drug discovery. *Expert Opinion on Drug Discovery* **5** (2010) 235-248.

[4] R. Mannhold, G.I. Poda, C. Ostermann, I.V. Tetko. Calculation of molecular lipophilicity: State-of-the-art and comparison of log P methods on more than 96,000 compounds. *J Pharm Sci* **98** (2009) 861-893.

[5] K. Valkó, C. Bevan, D. Reynolds. Chromatographic hydrophobicity index by fast-gradient RP-HPLC: a high-throughput alternative to log P/log D. *Analytical chemistry* **69** (1997) 2022-2029.

[6] F. Lombardo, M.Y. Shalaeva, K.A. Tupper, F. Gao. ElogDoct: A Tool for Lipophilicity Determination in Drug Discovery. 2. Basic and Neutral Compounds. *Journal of Medicinal Chemistry* **44** (2001) 2490-2497.

[7] C.A. Lipinski, F. Lombardo, B.W. Dominy, P.J. Feeney. Experimental and computational approaches to estimate solubility and permeability in drug discovery and development settings1PII of original article: S0169-409X(96)00423-1. The article was originally published in Advanced Drug Delivery Reviews 23 (1997) 3–25.1. *Advanced Drug Delivery Reviews* **46** (2001) 3-26.

[8] A.L. Hopkins, C.R. Groom, A. Alex. Ligand efficiency: a useful metric for lead selection. *Drug Discov Today* **9** (2004) 430-431.

[9] P.D. Leeson, B. Springthorpe. The influence of drug-like concepts on decision-making in medicinal chemistry. *Nat Rev Drug Discov* **6** (2007) 881-890.

[10] T. Ryckmans, M.P. Edwards, V.A. Horne, A.M. Correia, D.R. Owen, L.R. Thompson, I. Tran, M.F. Tutt, T. Young. Rapid assessment of a novel series of selective CB(2) agonists using parallel synthesis protocols: A Lipophilic Efficiency (LipE) analysis. *Bioorg Med Chem Lett* **19** (2009) 4406-4409.

[11] A.F. Stepan, G.W. Kauffman, C.E. Keefer, P.R. Verhoest, M. Edwards. Evaluating the Differences in Cycloalkyl Ether Metabolism Using the Design Parameter “Lipophilic Metabolism Efficiency” (LipMetE) and a Matched Molecular Pairs Analysis. *Journal of Medicinal Chemistry* **56** (2013) 6985-6990.

[12] T.T. Wager, X. Hou, P.R. Verhoest, A. Villalobos. Moving beyond Rules: The Development of a Central Nervous System Multiparameter Optimization (CNS MPO) Approach To Enable Alignment of Druglike Properties. *ACS Chemical Neuroscience* **1** (2010) 435-449.

[13] M.M. Claffey, C.J. Helal, P.R. Verhoest, Z. Kang, K.S. Fors, S. Jung, J. Zhong, M.W. Bundesmann, X. Hou, S. Lui, R.J. Kleiman, M. Vanase-Frawley, A.W. Schmidt, F. Menniti, C.J. Schmidt, W.E. Hoffman, M. Hajos, L. McDowell, R.E. O’Connor, M. MacDougall-Murphy, K.R. Fonseca, S.L. Becker, F.R. Nelson, S. Liras. Application of Structure-Based Drug Design and Parallel Chemistry to Identify

Selective, Brain Penetrant, In Vivo Active Phosphodiesterase 9A Inhibitors. *Journal of Medicinal Chemistry* **55** (2012) 9055-9068.

[14] M.P. Gleeson. Generation of a Set of Simple, Interpretable ADMET Rules of Thumb. *Journal of Medicinal Chemistry* **51** (2008) 817-834.

[15] M.V. Varma, R.S. Obach, C. Rotter, H.R. Miller, G. Chang, S.J. Steyn, A. El-Kattan, M.D. Troutman. Physicochemical space for optimum oral bioavailability: contribution of human intestinal absorption and first-pass elimination. *J Med Chem* **53** (2010) 1098-1108.

[16] T.W. Johnson, K.R. Dress, M. Edwards. Using the Golden Triangle to optimize clearance and oral absorption. *Bioorganic & Medicinal Chemistry Letters* **19** (2009) 5560-5564.

[17] A.L. Hopkins, G.M. Keserü, P.D. Leeson, D.C. Rees, C.H. Reynolds. The role of ligand efficiency metrics in drug discovery. *Nature Reviews Drug Discovery* **13** (2014) 105.

[18] J.S. Scott, M.J. Waring. Practical application of ligand efficiency metrics in lead optimisation. *Bioorganic & Medicinal Chemistry* (2018).

[19] R.J. Young, P.D. Leeson. Mapping the Efficiency and Physicochemical Trajectories of Successful Optimizations. *Journal of Medicinal Chemistry* (2018).

[20] T.W. Johnson, R.A. Gallego, M.P. Edwards. Lipophilic Efficiency as an Important Metric in Drug Design. *Journal of Medicinal Chemistry* (2018).

[21] C.R. Butler, E.M. Beck, A. Harris, Z. Huang, L.A. McAllister, C.W. am Ende, K. Fennell, T.L. Foley, K. Fonseca, S.J. Hawrylik, D.S. Johnson, J.D. Knafels, S. Mente, G.S. Noell, J. Pandit, T.B. Phillips, J.R. Piro, B.N. Rogers, T.A. Samad, J. Wang, S. Wan, M.A. Brodney. Azetidine and Piperidine Carbamates as Efficient, Covalent Inhibitors of Monoacylglycerol Lipase. *Journal of Medicinal Chemistry* **60** (2017) 9860-9873.

[22] M. Ammirati, S.W. Bagley, S.K. Bhattacharya, L. Buckbinder, A.A. Carlo, R. Conrad, C. Cortes, R.L. Dow, M.S. Dowling, A. El-Kattan, K. Ford, C.R.W. Guimarães, D. Hepworth, W. Jiao, J. LaPerle, S. Liu, A. Londregan, P.M. Loria, A.M. Mathiowetz, M. Munchhof, S.T.M. Orr, D.N. Petersen, D.A. Price, A. Skoura, A.C. Smith, J. Wang. Discovery of an in Vivo Tool to Establish Proof-of-Concept for MAP4K4-Based Antidiabetic Treatment. *ACS Medicinal Chemistry Letters* **6** (2015) 1128-1133.

[23] M. Pettersson, D.S. Johnson, C. Subramanyam, K.R. Bales, C.W. am Ende, B.A. Fish, M.E. Green, G.W. Kauffman, P.B. Mullins, T. Navaratnam, S.M. Sakya, C.M. Stiff, T.P. Tran, L. Xie, L. Zhang, L.R. Pustilnik, B.C. Vetelino, K.M. Wood, N. Pozdnyakov, P.R. Verhoest, C.J. O'Donnell. Design, Synthesis, and Pharmacological Evaluation of a Novel Series of Pyridopyrazine-1,6-dione γ-Secretase Modulators. *Journal of Medicinal Chemistry* **57** (2014) 1046-1062.

[24] C. Hansch, J.P. Bjorkroth, A. Leo. Hydrophobicity and central nervous system agents: on the principle of minimal hydrophobicity in drug design. *J Pharm Sci* **76** (1987) 663-687.

[25] L. Di, P. Artursson, A. Avdeef, G.F. Ecker, B. Faller, H. Fischer, J.B. Houston, M. Kansy, E.H. Kerns, S.D. Krämer. Evidence-based approach to assess passive diffusion and carrier-mediated drug transport. *Drug Discov Today* **17** (2012) 905-912.

[26] C.A. Lipinski, F. Lombardo, B.W. Dominy, P.J. Feeney. Experimental and computational approaches to estimate solubility and permeability in drug discovery and development settings1. *Advanced Drug Delivery Reviews* **23** (1997) 3-25.

[27] C.A. Lipinski, F. Lombardo, B.W. Dominy, P.J. Feeney. Experimental and computational approaches to estimate solubility and permeability in drug discovery and development settings. *Advanced Drug Delivery Reviews* **46** (2001) 3-26.

[28] M.E. Kavanagh, M.R. Doddareddy, M. Kassiou. The development of CNS-active LRRK2 inhibitors using property-directed optimisation. *Bioorganic & Medicinal Chemistry Letters* **23** (2013) 3690-3696.

[29] M.P. Deninno, M. Andrews, A.S. Bell, Y. Chen, C. Eller-Zarbo, N. Eshelby, J.B. Etienne, D.E. Moore, M.J. Palmer, M.S. Visser, L.J. Yu, W.J. Zavadoski, E. Michael Gibbs. The discovery of potent, selective, and orally bioavailable PDE9 inhibitors as potential hypoglycemic agents. *Bioorg Med Chem Lett* **19** (2009) 2537-2541.

[30] Z. Rankovic. CNS Physicochemical Property Space Shaped by a Diverse Set of Molecules with Experimentally Determined Exposure in the Mouse Brain. *J Med Chem* **60** (2017) 5943-5954.

[31] N.M. Ahmad. Solubility-driven lead optimisation: Recent examples and personal perspectives. *Bioorganic & Medicinal Chemistry Letters* **26** (2016) 2975-2979.

[32] D.J. Craik, D.P. Fairlie, S. Liras, D. Price. The future of peptide-based drugs. *Chem Biol Drug Des* **81** (2013) 136-147.

[33] K. Fosgerau, T. Hoffmann. Peptide therapeutics: current status and future directions. *Drug discovery today* **20** (2015) 122-128.

[34] M.E. Bunnage, E.L.P. Chekler, L.H. Jones. Target validation using chemical probes. *Nature Chemical Biology* **9** (2013) 195.

[35] C.R. Guimaraes, A.M. Mathiowetz, M. Shalaeva, G. Goetz, S. Liras. Use of 3D Properties to Characterize Beyond Rule-of-5 Property Space for Passive Permeation. *Journal of Chemical Information and Modeling* **52** (2012) 882-890.

[36] B.C. Doak, B. Over, F. Giordanetto, J. Kihlberg. Oral druggable space beyond the rule of 5: insights from drugs and clinical candidates. *Chem Biol* **21** (2014) 1115-1142.

[37] C.K. Wang, S.E. Northfield, J.E. Swedberg, B. Colless, S. Chaousis, D.A. Price, S. Liras, D.J. Craik. Exploring experimental and computational markers of cyclic peptides: charting islands of permeability. *Eur J Med Chem* **97** (2015) 202-213.

[38] A.T. Bockus, K.W. Lexa, C.R. Pye, A.S. Kalgutkar, J.W. Gardner, K.C.R. Hund, W.M. Hewitt, J.A. Schwochert, E. Glassey, D.A. Price, A.M. Mathiowetz, S. Liras, M.P. Jacobson, R.S. Lokey. Probing the Physicochemical Boundaries of Cell Permeability and Oral Bioavailability in Lipophilic Macrocycles Inspired by Natural Products. *Journal of Medicinal Chemistry* **58** (2015) 4581-4589.

[39] C.R. Pye, W.M. Hewitt, J.A. Schwochert, T.D. Haddad, C.E. Townsend, L. Etienne, Y. Lao, C. Limberakis, A. Furukawa, A.M. Mathiowetz, D.A. Price, S. Liras, R.S. Lokey. Non-Classical Size Dependence of Permeation Defines Bounds for Passive Adsorption of Large Drug Molecules. *Journal of Medicinal Chemistry* (2017).

[40] P. Seiler. Interconversion of lipophilicities from hydrocarbon/water systems into the octanol/water system. *Eur J Med Chem* **39** (1974) 473-479.

[41] T.W. von Geldern, D.J. Hoffman, J.A. Kester, H.N. Nellans, B.D. Dayton, S.V. Calzadilla, K.C. Marsh, L. Hernandez, W. Chiou, D.B. Dixon, J.R. Wu-Wong, T.J. Opgenorth. Azole Endothelin Antagonists. 3. Using Δ log P as a Tool To Improve Absorption. *Journal of Medicinal Chemistry* **39** (1996) 982-991.

[42] R.C. Young, R.C. Mitchell, T.H. Brown, C.R. Ganellin, R. Griffiths, M. Jones, K.K. Rana, D. Saunders, I.R. Smith. Development of a new physicochemical model for brain penetration and its application to the design of centrally acting H2 receptor histamine antagonists. *Journal of Medicinal Chemistry* **31** (1988) 656-671.

[43] J.T. Goodwin, R.A. Conradi, N.F. Ho, P.S. Burton. Physicochemical determinants of passive membrane permeability: role of solute hydrogen-bonding potential and volume. *J Med Chem* **44** (2001) 3721-3729.

[44] M.H. Abraham, R.E. Smith, R. Luchtefeld, A.J. Boorem, R. Luo, W.E. Acree, Jr. Prediction of solubility of drugs and other compounds in organic solvents. *J Pharm Sci* **99** (2010) 1500-1515.

[45] G. Gilli, P. Gilli, The Nature of the Hydrogen Bond: Outline of a Comprehensive Hydrogen Bond Theory Oxford University Press, New York2009.

[46] M. Shalaeva, G. Caron, Y.A. Abramov, T.N. O'Connell, M.S. Plummer, G. Yalamanchi, K.A. Farley, G.H. Goetz, L. Philippe, M.J. Shapiro. Integrating Intramolecular Hydrogen Bonding (IMHB) Considerations in Drug Discovery Using ΔlogP As a Tool. *Journal of Medicinal Chemistry* **56** (2013) 4870-4879.

[47] C.K. Wittekindt, A. COSMO-RS as a Predictive Tool for Lipophilicity. *QSAR Comb. Sci.* **28** (2009) 874–877.

[48] G. Caron, M. Vallaro, G. Ermondi, G.H. Goetz, Y.A. Abramov, L. Philippe, M. Shalaeva. A fast chromatographic method for estimating lipophilicity and ionization in nonpolar membrane-like environment. *Molecular Pharmaceutics* **13** (2016) 1100-1110.

[49] P. Saha, J.H. Kou. Effect of solubilizing excipients on permeation of poorly water-soluble compounds across Caco-2 cell monolayers. *European Journal of Pharmaceutics and Biopharmaceutics* **50** (2000) 403-411.

[50] K. Futatsugi, K.B. Bahnck, M.B. Brenner, J. Buxton, J.E. Chin, S.B. Coffey, J. Dubins, D. Flynn, D. Gautreau, A. Guzman-Perez, J.R. Hadcock, D. Hepworth, M. Herr, T. Hinchey, A.M. Janssen, S.M. Jennings, W. Jiao, S.Y. Lavergne, B. Li, M. Li, M.J. Munchhof, S.T.M. Orr, D.W. Piotrowski, N.S. Roush, M. Sammons, B.D. Stevens, G. Storer, J. Wang, J.S. Warmus, L. Wei, A.C. Wolford. Optimization of triazole-based TGR5 agonists towards orally available agents. *MedChemComm* **4** (2013) 205-210.

[51] M.J. Waring, J. Arrowsmith, A.R. Leach, P.D. Leeson, S. Mandrell, R.M. Owen, G. Pairaudeau, W.D. Pennie, S.D. Pickett, J. Wang, O. Wallace, A. Weir. An analysis of the attrition of drug candidates from four major pharmaceutical companies. *Nature Reviews Drug Discovery* **14** (2015) 475.

[52] J.D. Hughes, J. Blagg, D.A. Price, S. Bailey, G.A. Decrescenzo, R.V. Devraj, E. Ellsworth, Y.M. Fobian, M.E. Gibbs, R.W. Gilles, N. Greene, E. Huang, T. Krieger-Burke, J. Loesel, T. Wager, L. Whiteley, Y. Zhang. Physiochemical drug properties associated with in vivo toxicological outcomes. *Bioorg Med Chem Lett* **18** (2008) 4872-4875.

[53] D.A. Price, J. Blagg, L. Jones, N. Greene, T. Wager. Physicochemical drug properties associated with in vivo toxicological outcomes: a review. *Expert Opin Drug Metab Toxicol* **5** (2009) 921-931.

[54] M.C. Wenlock. Designing safer oral drugs. *MedChemComm* **8** (2017) 571-577.

[55] F. Lombardo, M.Y. Shalaeva, K.A. Tupper, F. Gao, M.H. Abraham. ElogPoct: A Tool for Lipophilicity Determination in Drug Discovery. *Journal of Medicinal Chemistry* **43** (2000) 2922-2928.

[56] Y. Gravenfors, J. Viklund, J. Blid, T. Ginman, S. Karlström, J. Kihlström, K. Kolmodin, J. Lindström, S. von Berg, F. von Kieseritzky, C. Slivo, B.-M. Swahn, L.-L. Olsson, P. Johansson, S. Eketjäll, J. Fälting, F. Jeppsson, K. Strömberg, J. Janson, F. Rahm. New Aminoimidazoles as β-Secretase (BACE-1) Inhibitors Showing Amyloid-β (Aβ) Lowering in Brain. *Journal of Medicinal Chemistry* **55** (2012) 9297-9311.

[57] P. Mukherjee, M. Pettersson, J.K. Dutra, L. Xie, C.W. Am Ende. Trifluoromethyl Oxetanes: Synthesis and Evaluation as a tert-Butyl Isostere. *ChemMedChem* **12** (2017) 1574-1577.

[58] A.F. Stepan, K. Karki, W.S. McDonald, P.H. Dorff, J.K. Dutra, K.J. Dirico, A. Won, C. Subramanyam, I.V. Efremov, C.J. O'Donnell, C.E. Nolan, S.L. Becker, L.R. Pustilnik, B. Sneed, H. Sun, Y. Lu, A.E. Robshaw, D. Riddell, T.J. O'Sullivan, E. Sibley, S. Capetta, K. Atchison, A.J. Hallgren, E. Miller, A. Wood, R.S. Obach. Metabolism-directed design of oxetane-containing arylsulfonamide derivatives as gamma-secretase inhibitors. *J Med Chem* **54** (2011) 7772-7783.

[59] D.A. Griffith, R.L. Dow, K. Huard, D.J. Edmonds, S.W. Bagley, J. Polivkova, D. Zeng, C.N. Garcia-Irizarry, J.A. Southers, W. Esler, P. Amor, K. Loomis, K. McPherson, K.B. Bahnck, C. Preville, T. Banks, D.E. Moore, A.M. Mathiowetz, E. Menhaji-Klotz, A.C. Smith, S.D. Doran, D.A. Beebe, M.F. Dunn. Spirolactam-based acetyl-CoA carboxylase inhibitors: toward improved metabolic stability of a chromanone lead structure. *J Med Chem* **56** (2013) 7110-7119.

[60] J.E. Davoren, C.W. Lee, M. Garnsey, M.A. Brodney, J. Cordes, K. Dlugolenski, J.R. Edgerton, A.R. Harris, C.J. Helal, S. Jenkinson, G.W. Kauffman, T.P. Kenakin, J.T. Lazzaro, S.M. Lotarski, Y. Mao, D.M. Nason, C. Northcott, L. Nottebaum, S.V. O'Neil, B. Pettersen, M. Popiolek, V. Reinhart, R. Salomon-Ferrer, S.J. Steyn, D. Webb, L. Zhang, S. Grimwood. Discovery of the Potent and Selective M1 PAM-Agonist N-[(3R,4S)-3-Hydroxytetrahydro-2H-pyran-4-yl]-5-methyl-4-[4-(1,3-thiazol-4-yl)ben zyl]pyridine-2-carboxamide (PF-06767832): Evaluation of Efficacy and Cholinergic Side Effects. *J Med Chem* **59** (2016) 6313-6328.

[61] A. Forsberg, A. Juréus, Z. Cselényi, M. Eriksdotter, Y. Freund-Levi, F. Jeppsson, B.-M. Swahn, J. Sandell, P. Julin, M. Schou, J. Andersson, P. Johnström, K. Varnäs, C. Halldin, L. Farde, S. Svensson. Low background and high contrast PET imaging of amyloid-β with [(11)C]AZD2995 and

[(11)C]AZD2184 in Alzheimer's disease patients. *European Journal of Nuclear Medicine and Molecular Imaging* **40** (2013) 580-593.

[62] K. Palm, K. Luthman, A.L. Ungell, G. Strandlund, P. Artursson. Correlation of drug absorption with molecular surface properties. *J Pharm Sci* **85** (1996) 32-39.

[63] H. van De Waterbeemd, G. Camenisch, G. Folkers, O.A. Raevsky. Estimation of Caco-2 Cell Permeability using Calculated Molecular Descriptors. *Quantitative Structure-Activity Relationships* **15** (1996) 480-490.

[64] Y.H. Zhao, M.H. Abraham, A. Ibrahim, P.V. Fish, S. Cole, M.L. Lewis, M.J. de Groot, D.P. Reynolds. Predicting penetration across the blood-brain barrier from simple descriptors and fragmentation schemes. *J Chem Inf Model* **47** (2007) 170-175.

[65] K. Palm, P. Stenberg, K. Luthman, P. Artursson1. Polar Molecular Surface Properties Predict the Intestinal Absorption of Drugs in Humans. *Pharm Res* **14** (1997) 568-571.

[66] D.E. Clark. Rapid calculation of polar molecular surface area and its application to the prediction of transport phenomena. 1. Prediction of intestinal absorption. *J Pharm Sci* **88** (1999) 807-814.

[67] D.E. Clark. Rapid calculation of polar molecular surface area and its application to the prediction of transport phenomena. 2. Prediction of blood-brain barrier penetration. *J Pharm Sci* **88** (1999) 815-821.

[68] S. Winiwarter, N.M. Bonham, F. Ax, A. Hallberg, H. Lennernas, A. Karlen. Correlation of human jejunal permeability (in vivo) of drugs with experimentally and theoretically derived parameters. A multivariate data analysis approach. *J Med Chem* **41** (1998) 4939-4949.

[69] J. Kelder, P.D. Grootenhuis, D.M. Bayada, L.P. Delbressine, J.P. Ploemen. Polar molecular surface as a dominating determinant for oral absorption and brain penetration of drugs. *Pharm Res* **16** (1999) 1514-1519.

[70] L.H. Krarup, I.T. Christensen, L. Hovgaard, S. Frokjaer. Predicting drug absorption from molecular surface properties based on molecular dynamics simulations. *Pharm Res* **15** (1998) 972-978.

[71] P. Ertl, B. Rohde, P. Selzer. Fast calculation of molecular polar surface area as a sum of fragment-based contributions and its application to the prediction of drug transport properties. *J Med Chem* **43** (2000) 3714-3717.

[72] P. Ertl, Polar Surface Area, Molecular Drug Properties, Wiley-VCH Verlag GmbH & Co. KGaA2008, pp. 111-126.

[73] G. Schaftenaar, J. de Vlieg. Quantum mechanical polar surface area. *Journal of Computer-Aided Molecular Design* **26** (2012) 311-318.

[74] S. Prasanna, R.J. Doerksen. Topological polar surface area: a useful descriptor in 2D-QSAR. *Curr Med Chem* **16** (2009) 21-41.

[75] J. Fernandes, C.R. Gattass. Topological polar surface area defines substrate transport by multidrug resistance associated protein 1 (MRP1/ABCC1). *J Med Chem* **52** (2009) 1214-1218.

[76] D.F. Veber, S.R. Johnson, H.Y. Cheng, B.R. Smith, K.W. Ward, K.D. Kopple. Molecular properties that influence the oral bioavailability of drug candidates. *J Med Chem* **45** (2002) 2615-2623.

[77] H. van de Waterbeemd, G. Camenisch, G. Folkers, J.R. Chretien, O.A. Raevsky. Estimation of blood-brain barrier crossing of drugs using molecular size and shape, and H-bonding descriptors. *J Drug Target* **6** (1998) 151-165.

[78] T.T. Wager, X. Hou, P.R. Verhoest, A. Villalobos. Central Nervous System Multiparameter Optimization Desirability: Application in Drug Discovery. *ACS Chem Neurosci* **7** (2016) 767-775.

[79] J. Drews. Stategic trends in the drug industry. *Drug Discov Today* **8** (2003) 411-420.

[80] G.H. Goetz, W. Farrell, M. Shalaeva, S. Sciabola, D. Anderson, J. Yan, L. Philippe, M.J. Shapiro. High throughput method for the indirect detection of intramolecular hydrogen bonding. *Journal of Medicinal Chemistry* **57** (2014) 2920-2929.

[81] A. Alex, D.S. Millan, M. Perez, F. Wakenhut, G.A. Whitlock. Intramolecular hydrogen bonding to improve membrane permeability and absorption in beyond rule of five chemical space. *MedChemComm* **2** (2011) 669-674.

[82] B. Kuhn, P. Mohr, M. Stahl. Intramolecular hydrogen bonding in medicinal chemistry. *Journal of Medicinal Chemistry* **53** (2010) 2601-2611.

[83] S.B. Rafi, B.R. Hearn, P. Vedantham, M.P. Jacobson, A.R. Renslo. Predicting and Improving the Membrane Permeability of Peptidic Small Molecules. *Journal of Medicinal Chemistry* **55** (2012) 3163-3169.

[84] T. Rezai, J.E. Bock, M.V. Zhou, C. Kalyanaraman, R.S. Lokey, M.P. Jacobson. Conformational Flexibility, Internal Hydrogen Bonding, and Passive Membrane Permeability: Successful in Silico Prediction of the Relative Permeabilities of Cyclic Peptides. *Journal of the American Chemical Society* **128** (2006) 14073-14080.

[85] T. Rezai, B. Yu, G.L. Millhauser, M.P. Jacobson, R.S. Lokey. Testing the conformational hypothesis of passive membrane permeability using synthetic cyclic peptide diastereomers. *J Am Chem Soc* **128** (2006) 2510-2511.

[86] H. Cheng, J.E. Hoffman, P.T. Le, M. Pairish, R. Kania, W. Farrell, S. Bagrodia, J. Yuan, S. Sun, E. Zhang, C. Xiang, D. Dalvie, S.V. Rahavendran. Structure-based design, SAR analysis and antitumor activity of PI3K/mTOR dual inhibitors from 4-methylpyridopyrimidinone series. *Bioorganic & Medicinal Chemistry Letters* **23** (2013) 2787-2792.

[87] F. Wakenhut, T.D. Tran, C. Pickford, S. Shaw, M. Westby, C. Smith-Burchnell, L. Watson, M. Paradowski, J. Milbank, D. Stonehouse, K. Cheung, R. Wybrow, F. Daverio, S. Crook, K. Statham, D. Leese, D. Stead, F. Adam, D. Hay, L.R. Roberts, J.Y. Chiva, C. Nichols, D.C. Blakemore, G.H. Goetz, Y. Che, I. Gardner, S. Dayal, A. Pike, R. Webster, D.C. Pryde. The discovery of potent nonstructural protein 5A (NS5A) inhibitors with a unique resistance profile-Part 2. *ChemMedChem* **9** (2014) 1387-1396.

[88] G.H. Goetz, L. Philippe, M.J. Shapiro. EPSA: A novel supercritical fluid chromatography technique enabling the design of permeable cyclic peptides. *ACS Medicinal Chemistry Letters* **5** (2014) 1167-1172.

[89] D.S. Nielsen, H.N. Hoang, R.J. Lohman, T.A. Hill, A.J. Lucke, D.J. Craik, D.J. Edmonds, D.A. Griffith, C.J. Rotter, R.B. Ruggeri. Improving on nature: making a cyclic heptapeptide orally bioavailable. *Angewandte Chemie International Edition* **53** (2014) 12059-12063.

[90] J. Schwochert, R. Turner, M. Thang, R.F. Berkeley, A.R. Ponkey, K.M. Rodriguez, S.S. Leung, B. Khunte, G. Goetz, C. Limberakis. Peptide to peptoid substitutions increase cell permeability in cyclic hexapeptides. *Organic letters* **17** (2015) 2928-2931.

[91] S. Sciabola, G.H. Goetz, G. Bai, B.N. Rogers, D.L. Gray, A. Duplantier, K.R. Fonseca, M.A. Vanase-Frawley, N.M. Kablaoui. Systematic N-methylation of oxytocin: Impact on pharmacology and intramolecular hydrogen bonding network. *Bioorganic & Medicinal Chemistry* **24** (2016) 3513-3520.

[92] S.G. Sciabola, Gilles ; Farrell, William High-Throughput Method for the Indirect Detection of IMHB. SSC14 - 14th Scandinavian Symposium on Chemometrics 2015Sardinia, Italy, 2015.

[93] G. Goetz. EPSA: A Novel Supercritical Fluid Chromatography Technique Enabling the Design of Permeable Cyclic Peptides. World Preclinical CongressBoston, 2016.

[94] D.A. DeGoey, H.-J. Chen, P.B. Cox, M.D. Wendt. Beyond the Rule of 5: Lessons Learned from AbbVie's Drugs and Compound Collection: Miniperspective. *Journal of Medicinal Chemistry* (2017).

[95] T. Vorherr, I. Lewis, J. Berghausen, S. Desrayaud, M. Schaefer. Modulation of oral bioavailability and metabolism for closely related cyclic hexapeptides. *International Journal of Peptide Research and Therapeutics* (2017) 1-14.

[96] S.C. Ha, Seth Optimizing Permeability of Peptides. Computational Drug DevelopmentBoston, 2015.

[97] J.P.L. Kiplinger, P. M.; Rego, M. J.; Rouse, E. S. . EPSA: A New Bioavailability / Permeability Assay. in: http://www.avericadiscovery.com/blog/epsa/ (Ed.), 2015.

[98] P. Wipf. ACS Medicinal Chemistry Letters: Technology Notes. *ACS Medicinal Chemistry Letters* **8** (2017) 1-2.